

Synthesis and Photophysical Properties of Silicon Phthalocyanines with Axial Siloxy Ligands Bearing Alkylamine Termini

H. M. Anula,[†] Jeffrey C. Berlin,[‡] Hongqiao Wu,[‡] Ying-Syi Li,[‡] Xingzhan Peng,[‡] Malcolm E. Kenney,^{*,‡} and Michael A. J. Rodgers^{*,†}

Center for Photochemical Sciences and Department of Chemistry, Bowling Green State University, Bowling Green, Ohio 43403, and Department of Chemistry, Case Western Reserve University, Cleveland, Ohio 44106

Received: October 31, 2005; In Final Form: February 13, 2006

Eleven silicon phthalocyanines which can be grouped into two homologous series [SiPc[OSi(CH₃)₂(CH₂)_nN(CH₃)₂]₂, *n* = 1–6 (series 1), and SiPc[OSi(CH₃)₂(CH₂)₃N((CH₂)_nH)₂]₂, *n* = 1–6 (series 2)] as well as an analogous phthalocyanine, SiPc[OSi(CH₃)₂(CH₂)₃NH₂]₂, were synthesized. The ground state absorption spectra, the triplet state dynamics, and singlet oxygen quantum yields of 10 of these phthalocyanines were measured. All compounds displayed similar ground state absorption spectral properties in dimethylformamide solution with single Q band maxima at 668 ± 2 nm and B band maxima at 352 ± 1 nm. Photoexcitation of all compounds in the B bands generated the optical absorptions of the triplet states which decayed with lifetimes in the hundreds of microseconds region. Oxygen quenching bimolecular rate constants near 2 × 10⁹ M⁻¹ s⁻¹ were measured, indicating that energy transfer to oxygen was exergonic. Singlet oxygen quantum yields, Φ_Δ, were measured, and those phthalocyanines in which the axial ligands are terminated by dimethylamine residues at the end of alkyl chains having four or more methylene links exhibited yields near ≥0.35. Others gave singlet oxygen quantum yields near 0.2, and still others showed singlet oxygen yields of <0.1. The reduced singlet oxygen yields are probably caused by a charge transfer quenching of the ¹π,π* state of the phthalocyanine by interaction with the lone pair electrons on the nitrogen atoms of the amine termini. In some cases, these can approach and interact with the electronically excited π-framework, owing to diffusive motions of the flexible oligo-methylene tether.

Introduction

Singlet molecular oxygen, O₂(¹Δ_g), is a metastable excited state of ground state molecular oxygen, O₂(³Σ_g⁻). It has received increasing attention as a reactive intermediate in a variety of photochemical, photobiological, enzymatic, and environmental processes.¹ It is believed that O₂(¹Δ_g) is involved in biological oxidative processes causing cytotoxic damage in living systems.² Furthermore, O₂(¹Δ_g) is generally accepted to be a key intermediate in photodynamic therapy (PDT). The production of the excited state of molecular oxygen, O₂(¹Δ_g), via the so-called type II pathway involves energy transfer from an electronically excited triplet state of sensitizer molecule S to the ground state of molecular oxygen, O₂(³Σ_g⁻). A current growth area in research related to photodynamic tumor therapy (PDT) involves the search for and characterization of photosensitizers that improve upon the presently used hematoporphyrin derivative (HpD, Photofrin). One basic requirement of a PDT photosensitizer is that it should have optimal light absorbing properties in the therapeutic window; that of HpD in the therapeutic window is very weak. There is a wide range of potential photosensitizers that have much better absorbing characteristics than HpD, and some work has already been carried out on molecules such as chlorins³ and phthalocyanines.⁴

In our laboratories and in a few others, the focus has been on the synthesis of phthalocyanines (Pc) having potential for

use in PDT and on evaluation of their photosensitizing efficiency. These compounds have absorption spectra that show maxima in the red spectral region with extinction coefficients in excess of 10⁵ M⁻¹ cm⁻¹. With all other things being equal, phthalocyanines should prove to have higher efficiencies as PDT sensitizers than do the members of the porphyrin family. The group IV metal phthalocyanines are of particular interest for PDT partly because their axial ligands can be varied and thus their properties tuned. As a part of our work, 11 silicon phthalocyanines having amino-terminated alkylsiloxy axial ligands have been synthesized. These 11 phthalocyanines can be grouped into two homologous series. One, series 1, has compounds with from one to six carbon atoms in its linker chains, and the second, series 2, has compounds with from one to six carbon atoms in its terminal-group chains (one compound is common to both series) (Figure 1). The members of series 1 are SiPc[OSi(CH₃)₂(CH₂)_nN(CH₃)₂]₂, *n* = 1–6, and those of series 2 are SiPc[OSi(CH₃)₂(CH₂)₃N((CH₂)_nH)₂]₂, *n* = 1–6. The compound SiPc[OSi(CH₃)₂(CH₂)₃NH₂]₂, an analogue (but not a homologue) of the members of series 2, has also been synthesized. The photophysical properties of 10 of these phthalocyanines have been studied and are reported herein.

Experimental Section

Materials for Photochemical Studies. Toluene, dimethylformamide (DMF), and benzene (spectrophotometric grade) were purchased from Aldrich. Tetraphenylporphyrin (TPP) was purchased from Porphyrin Products (now Frontier Scientific). SiPc(OH)₂ is available from Aldrich.

* To whom correspondence should be addressed. E-mail: malcolm.kenney@case.edu (M.E.K.); rogers@bgnnet.bgsu.edu (M.A.J.R.).

[†] Bowling Green State University.

[‡] Case Western Reserve University.

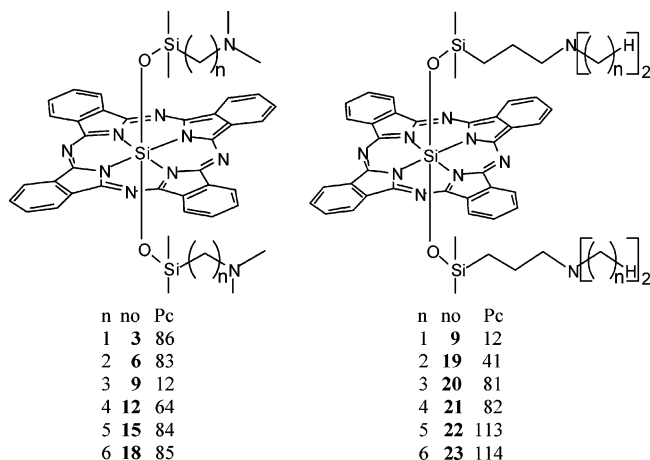


Figure 1. Structures of the linker-group, series 1, and terminal-group, series 2, phthalocyanines.

Syntheses. Linker-Group Phthalocyanines, Series 1, and Their Precursors. $\text{SiPc}[\text{OSi}(\text{CH}_3)_2(\text{CH}_2)_n\text{N}(\text{CH}_3)_2]_2$, $n = 1-6$. Ligand **1** was purchased, ligand **4** was made by a method designed specifically for it, and ligands **10**, **13**, and **16** were made in the same general manner as ligand **7**. Intermediate phthalocyanines **2**, **5**, **11**, **14**, and **17** were made in the same general manner as intermediate phthalocyanine **8** except that xylenes were used as the reaction solvent for **11**, **14**, and **17**, and linker-group phthalocyanines **3**, **6**, **12**, **15**, and **18** were made in the same general manner as linker-group phthalocyanine **9** except that a 1.0 M amine-tetrahydrofuran solution was used for **3**. Full descriptions of the syntheses are available in the Ph.D. thesis of J.C.B.⁵

$\text{ClSi}(\text{CH}_3)_2\text{CH}_2\text{Br}$, **1**. Purchased (Gelest, Morrisville, PA). NMR (CDCl_3): δ 2.63 (s, 2H, CH_2), 0.56 (s, 6H, SiCH_3). **1** is a colorless, mobile liquid. It is soluble in CH_2Cl_2 , toluene, and hexanes.

$\text{SiPc}[\text{OSi}(\text{CH}_3)_2\text{CH}_2\text{Br}]_2$, **2**. 78%. NMR (C_6D_6): δ 9.72 (m, 8H, 1,4-Pc H), 7.87 (m, 8H, 2,3-Pc H), -0.46 (s, 4H, SiCH_2), -2.61 (s, 12H, SiCH_3). **2** is a blue solid. It is moderately soluble in CH_2Cl_2 , dimethylformamide, and toluene and insoluble in hexanes.

$\text{SiPc}[\text{OSi}(\text{CH}_3)_2\text{CH}_2\text{N}(\text{CH}_3)_2]_2$, Pc 86, **3**. 65%. UV-vis (toluene) λ_{max} , nm (log ϵ): 670 (5.4). NMR (C_6D_6): δ 9.72 (m, 8H, 1,4-Pc H), 7.88 (m, 8H, 2,3-Pc H), 0.52 (s, 12H, NCH_3), -0.80 (t, 4H, SiCH_2), -2.55 (s, 12H, SiCH_3). HRMS-FAB (m/z): $(M + H)^+$ calcd for $\text{C}_{42}\text{H}_{44}\text{N}_{10}\text{O}_2\text{Si}_3$, 805.3035; found, 805.3061, 805.3025. **3** is a blue-green solid. It is moderately soluble in CH_2Cl_2 , dimethylformamide, and toluene and insoluble in hexanes.

$\text{ClSi}(\text{CH}_3)_2(\text{CH}_2)_2\text{Br}$, **4**. Under Ar, a cool (-5°C) solution of $(\text{Cl})_3\text{Si}(\text{CH}_2)_2\text{Br}$ (7.2 mL) and ether (75 mL) was treated dropwise with a CH_3MgBr -diethyl ether solution (3.0 M, 42 mL) at a rate of <5 mL/h and then with a solution of $\text{ClSi}(\text{CH}_3)_3$ (2.5 mL), tetrahydrofuran (25 mL), and diethyl ether (25 mL). The reaction product was separated by decantation, and the solid was washed (tetrahydrofuran-diethyl ether solution, 1:1). The decantate and washings were combined, vacuum concentrated (room temperature), and distilled twice (0.1 Torr, room temperature; 40 Torr, $60-70^\circ\text{C}$) and weighed (1.9 g, 25%). NMR (CDCl_3): δ 3.58 (t, 2H, SiCH_2CH_2), 1.62 (t, 2H, SiCH_2), 0.45 (s, 6H, SiCH_3). **4** is a colorless, mobile liquid. It is soluble in CH_2Cl_2 , toluene, and hexanes.

$\text{SiPc}[\text{OSi}(\text{CH}_3)_2(\text{CH}_2)_2\text{Br}]_2$, **5**. 38%. NMR (C_6D_6): δ 9.73 (m, 8H, 1,4-Pc H), 7.88 (m, 8H, 2,3-Pc H), 0.89 (m, 4H, SiCH_2CH_2), -1.46 (t, 4H, SiCH_2), -2.81 (s, 12H, SiCH_3). **5** is

a blue solid. It is soluble in CH_2Cl_2 , dimethylformamide, and toluene and slightly soluble in hexanes.

$\text{SiPc}[\text{OSi}(\text{CH}_3)_2(\text{CH}_2)_2\text{N}(\text{CH}_3)_2]_2$, Pc 83, **6**. 62%. UV-vis (toluene) λ_{max} , nm (log ϵ): 668 (5.4). NMR (C_6D_6): δ 9.72 (m, 8H, 1,4-Pc H), 7.87 (m, 8H, 2,3-Pc H), 1.24 (s, 12H, NCH_3), -0.22 (t, 4H, SiCH_2CH_2), -1.81 (t, 4H, SiCH_2), -2.62 (s, 12H, SiCH_3). HRMS-FAB (m/z): $(M + H)^+$ calcd for $\text{C}_{44}\text{H}_{48}\text{N}_{10}\text{O}_2\text{Si}_3$, 833.3347; found, 833.3318, 833.3339. **6** is a blue solid. It is soluble in CH_2Cl_2 , dimethylformamide, and toluene and insoluble in hexanes.

$\text{ClSi}(\text{CH}_3)_2(\text{CH}_2)_3\text{Br}$, **7**. Under Ar, a mixture of $\text{ClSi}(\text{CH}_3)_2\text{H}$ (25.0 g), allyl bromide (6.99 g), and platinum divinyltetramethyldisiloxane complex (Gelest, 2-3% Pt in xylenes, 12.8 mg) in a pressure tube was warmed ($\sim 60^\circ\text{C}$) for 3 days. The reaction product was distilled under Ar ($162-164^\circ\text{C}$), and the distillate was weighed (6.83 g). NMR (CDCl_3): δ 3.41 (t, 2H, $\text{Si}(\text{CH}_2)_2\text{CH}_2$), 1.92 (m, 2H, SiCH_2CH_2), 0.93 (t, 2H, SiCH_2), 0.41 (s, 6H, SiCH_3). **7** is a colorless, mobile liquid. It is soluble in CH_2Cl_2 , toluene, and hexanes. By NMR spectra, the product contains $\sim 20\%$ $\text{BrSi}(\text{CH}_3)_2(\text{CH}_2)_3\text{Br}$. Apparently, this also reacts with $\text{SiPc}(\text{OH})_2$ to give **8**.

$\text{SiPc}[\text{OSi}(\text{CH}_3)_2(\text{CH}_2)_3\text{Br}]_2$, Pc 145, **8**. A mixture of $\text{SiPc}(\text{OH})_2$ (259 mg) and toluene (120 mL) was dried by distillation (1 mL of distillate), treated sequentially with 2,6-di-*tert*-butylpyridine (562 mg) and silane **7** (507 mg), distilled for 4 h (9 mL of distillate), and filtered. The filtrate was evaporated to dryness by rotary evaporation (room temperature), and the solid was washed (CH_3CN), vacuum-dried (room temperature), and weighed (345 mg). NMR (C_6D_6): δ 9.74 (m, 8H, 1,4-Pc H), 7.90 (m, 8H, 2,3-Pc H), 1.71 (t, 4H, $\text{Si}(\text{CH}_2)_2\text{CH}_2$), -0.83 (m, 4H, SiCH_2CH_2), -2.30 (t, 4H, SiCH_2), -2.72 (s, 12H, SiCH_3). HRMS-FAB (m/z): $(M + H)^+$ calcd for $\text{C}_{42}\text{H}_{40}\text{Br}_2\text{N}_8\text{O}_2\text{Si}_3$, 931.1027; found, 931.0976, 931.0972. **8** is a blue solid. It is soluble in CH_2Cl_2 , dimethylformamide, and toluene and moderately soluble in hexanes.

$\text{SiPc}[\text{OSi}(\text{CH}_3)_2(\text{CH}_2)_3\text{N}(\text{CH}_3)_2]_2$, Pc 12, **9**. A mixture of phthalocyanine **8** (345 mg) and a dimethylamine-tetrahydrofuran solution (2.0 M, 9.7 mL) in a pressure tube was warmed ($\sim 60^\circ\text{C}$) for 72 h, passed down an Al_2O_3 column (basic Al_2O_3 V, CH_2Cl_2), and diluted with tetrahydrofuran (4.8 mL). The product was evaporated to dryness by rotary evaporation (room temperature), and the solid was washed (CH_3CN), air-dried (room temperature), and weighed (227 mg, 0.263 mmol, 69%). UV-vis (toluene) λ_{max} , nm (log ϵ): 668 (5.5). NMR (C_6D_6): δ 9.72 (m, 8H, 1,4-Pc H), 7.88 (m, 8H, 2,3-Pc H), 1.57 (s, 12H, NCH_3), 0.85 (t, 4H, $\text{Si}(\text{CH}_2)_2\text{CH}_2$), -0.92 (m, 4H, SiCH_2CH_2), -2.08 (t, 4H, SiCH_2), -2.62 (s, 12H, SiCH_3). **9** is a blue solid. It is soluble in CH_2Cl_2 , dimethylformamide, and toluene and insoluble in hexanes.

$\text{ClSi}(\text{CH}_3)_2(\text{CH}_2)_4\text{Br}$, **10**. 89%. NMR (CDCl_3): δ 3.41 (t, 2H, $\text{Si}(\text{CH}_2)_3\text{CH}_2$), 1.90 (m, 2H, $\text{Si}(\text{CH}_2)_2\text{CH}_2$), 1.56 (m, 2H, SiCH_2CH_2), 0.81 (t, 2H, SiCH_2), 0.40 (s, 6H, SiCH_3). **10** is a colorless, mobile liquid. It is soluble in CH_2Cl_2 , toluene, and hexanes.

$\text{SiPc}[\text{OSi}(\text{CH}_3)_2(\text{CH}_2)_4\text{Br}]_2$, **11**. 71%. NMR (C_6D_6): δ 9.72 (m, 8H, 1,4-Pc H), 7.90 (m, 8H, 2,3-Pc H), 2.21 (t, 4H, $\text{Si}(\text{CH}_2)_3\text{CH}_2$), 0.24 (m, 4H, $\text{Si}(\text{CH}_2)_2\text{CH}_2$), -1.24 (m, 4H, SiCH_2CH_2), -2.31 (t, 4H, SiCH_2), -2.67 (s, 12H, SiCH_3). **11** is a blue solid. It is soluble in CH_2Cl_2 , dimethylformamide, toluene, and hexanes.

$\text{SiPc}[\text{OSi}(\text{CH}_3)_2(\text{CH}_2)_4\text{N}(\text{CH}_3)_2]_2$, Pc 64, **12**. 51%. UV-vis (toluene) λ_{max} , nm (log ϵ): 668 (5.5). NMR (C_6D_6): δ 9.72 (m, 8H, 1,4-Pc H), 7.88 (m, 8H, 2,3-Pc H), 1.85 (s, 12H, NCH_3), 1.30 (t, 4H, $\text{Si}(\text{CH}_2)_3\text{CH}_2$), 0.15 (m, 4H, $\text{Si}(\text{CH}_2)_2\text{CH}_2$), -1.11

(m, 4H, SiCH₂CH₂), -2.10 (t, 4H, SiCH₂), -2.62 (s, 12H, SiCH₃). HRMS-FAB (*m/z*): (M + H)⁺ calcd for C₄₈H₅₆N₁₀O₂-Si₃, 889.3974; found, 889.3998, 889.3957. **12** is a blue solid. It is soluble in CH₂Cl₂, dimethylformamide, and toluene and insoluble in hexanes.

ClSi(CH₃)₂(CH₂)₅Br, **13**. 58%. NMR (CDCl₃): δ 3.42 (t, 2H, Si(CH₂)₄CH₂), 1.80 (m, 2H, Si(CH₂)₃CH₂), 1.46 (m, 4H, SiCH₂CH₂CH₂), 0.82 (t, 2H, SiCH₂), 0.41 (s, 6H, SiCH₃). **13** is a colorless, mobile liquid. It is soluble in CH₂Cl₂, toluene, and hexanes.

SiPc[OSi(CH₃)₂(CH₂)₅Br]₂, **14**. 83%. NMR (C₆D₆): δ 9.74 (m, 8H, 1,4-Pc H), 7.91 (m, 8H, 2,3-Pc H), 2.64 (t, 4H, Si(CH₂)₄CH₂), 0.74 (m, 4H, Si(CH₂)₃CH₂), -0.22 (m, 4H, Si(CH₂)₂CH₂), -1.35 (m, 4H, SiCH₂CH₂), -2.21 (t, 4H, SiCH₂), -2.64 (s, 12H, SiCH₃). **14** is a blue solid. It is soluble in CH₂-Cl₂, dimethylformamide, toluene, and hexanes.

SiPc[OSi(CH₃)₂(CH₂)₅N(CH₃)₂]₂, Pc 84, **15**. 73%. UV-vis (toluene) λ_{max}, nm (log ε): 668 (5.5). NMR (C₆D₆): δ 9.73 (m, 8H, 1,4-Pc H), 7.89 (m, 8H, 2,3-Pc H), 2.03 (s, 12H, NCH₃), 1.73 (t, 4H, Si(CH₂)₄CH₂), 0.62 (m, 4H, Si(CH₂)₃CH₂), -0.04 (m, 4H, Si(CH₂)₂CH₂), -1.13 (m, 4H, SiCH₂CH₂), -2.09 (t, 4H, SiCH₂), -2.62 (s, 12H, SiCH₃). HRMS-FAB (*m/z*): (M)⁺ calcd for C₅₀H₆₀N₁₀O₂Si₃, 916.4208; found, 916.4195, 916.4203. **15** is a blue solid. It is soluble in CH₂Cl₂, dimethylformamide, and toluene and slightly soluble in hexanes.

ClSi(CH₃)₂(CH₂)₆Br, **16**. 83%. NMR (CDCl₃): δ 3.39 (t, 2H, Si(CH₂)₅CH₂), 1.84 (m, 2H, Si(CH₂)₄CH₂), 1.38 (m, 6H, SiCH₂CH₂CH₂CH₂), 0.79 (t, 2H, SiCH₂), 0.38 (s, 6H, SiCH₃). **16** is a colorless, mobile liquid. It is soluble in CH₂Cl₂, toluene, and hexanes.

SiPc[OSi(CH₃)₂(CH₂)₆Br]₂, **17**. 72%. NMR (C₆D₆): δ 9.73 (m, 8H, 1,4-Pc H), 7.88 (m, 8H, 2,3-Pc H), 2.85 (t, 4H, Si(CH₂)₅CH₂), 1.09 (m, 4H, Si(CH₂)₄CH₂), 0.29 (m, 4H, Si(CH₂)₃CH₂), -0.30 (m, 4H, Si(CH₂)₂CH₂), -1.26 (m, 4H, SiCH₂CH₂), -2.14 (t, 4H, SiCH₂), -2.62 (s, 12H, SiCH₃). **17** is a blue solid. It is soluble in CH₂Cl₂, dimethylformamide, toluene, and hexanes.

SiPc[OSi(CH₃)₂(CH₂)₆N(CH₃)₂]₂, Pc 85, **18**. 45%. UV-vis (toluene) λ_{max}, nm (log ε): 668 (5.5). NMR (C₆D₆): δ 9.73 (m, 8H, 1,4-Pc H), 7.90 (m, 8H, 2,3-Pc H), 2.12 (s, 12H, NCH₃), 1.99 (t, 4H, Si(CH₂)₅CH₂), 1.01 (m, 4H, Si(CH₂)₄CH₂), 0.44 (m, 4H, Si(CH₂)₃CH₂), -0.07 (m, 4H, Si(CH₂)₂CH₂), -1.12 (m, 4H, SiCH₂CH₂), -2.08 (t, 4H, SiCH₂), -2.61 (s, 12H, SiCH₃). HRMS-FAB (*m/z*): (M)⁺ calcd for C₅₂H₆₄N₁₀O₂Si₃, 944.4521; found, 944.4532, 944.4527. **18** is a blue solid. It is soluble in CH₂Cl₂, dimethylformamide, toluene, and hexanes.

Terminal-Group Phthalocyanines, Series 2. SiPc[OSi(CH₃)₂(CH₂)₃N((CH₂)_nH)₂]₂, *n* = 1–6. Terminal-group phthalocyanines **19**–**23** were prepared in the same general way as described below for terminal-group (and linker-group) phthalocyanine **9** except that the reaction mixtures were heated (80–195 °C) and the reaction times were shorter. For **20**–**23**, the reaction pressure was atmospheric. Full details are available in the Ph.D. thesis of J.C.B.⁵

SiPc[OSi(CH₃)₂(CH₂)₃N(CH₃)₂]₂, Pc 12, **9**. Under Ar, a mixture of phthalocyanine **8** (330 mg) and dimethylamine (9.2 mL) in a pressure tube was kept at room temperature for 3 days and allowed to evaporate to dryness (room temperature). The solid was passed down an Al₂O₃ column (basic Al₂O₃ V, CH₂-Cl₂), and the product was evaporated to dryness by rotary evaporation (room temperature). The solid was chromatographed (basic Al₂O₃ III, CH₂Cl₂–tetrahydrofuran solution, 50:1), washed (ethanol–H₂O solution, 10:1), vacuum-dried (100 °C), and weighed (197 mg, 65%).

SiPc[OSi(CH₃)₂(CH₂)₃N((CH₂)₂H)₂]₂, Pc 41, **19**. 74%. UV-vis (toluene) λ_{max}, nm (log ε): 669 (5.4). NMR (C₆D₆): δ 9.72 (m, 8H, 1,4-Pc H), 7.88 (m, 8H, 2,3-Pc H), 1.88 (m, 8H, NCH₂), 1.07 (t, 4H, Si(CH₂)₂CH₂), 0.64 (m, 12H, NCH₂CH₃), -0.91 (m, 4H, SiCH₂CH₂), -2.09 (m, 4H, SiCH₂), -2.62 (s, 12H, SiCH₃). HRMS-FAB (*m/z*): (M + H)⁺ calcd for C₅₀H₆₀N₁₀O₂-Si₃, 917.4287; found, 917.4300, 917.4306. **19** is a blue solid. It is soluble in CH₂Cl₂, dimethylformamide, and toluene and insoluble in hexanes.

SiPc[OSi(CH₃)₂(CH₂)₃N((CH₂)₃H)₂]₂, Pc 81, **20**. 62%. UV-vis (toluene) λ_{max}, nm (log ε): 669 (5.5). NMR (C₆D₆): δ 9.72 (m, 8H, 1,4-Pc H), 7.89 (m, 8H, 2,3-Pc H), 1.76 (t, 8H, NCH₂), 1.02 (m, 12H, NCH₂CH₂ and Si(CH₂)₂CH₂), 0.68 (t, 12H, N(CH₂)₂CH₃), -0.88 (m, 4H, SiCH₂CH₂), -2.08 (t, 4H, SiCH₂), -2.61 (s, 12H, SiCH₃). HRMS-FAB (*m/z*): (M + H)⁺ calcd for C₅₄H₆₈N₁₀O₂Si₃, 973.4913; found, 973.4905, 973.4919. **20** is a blue solid. It is soluble in CH₂Cl₂, dimethylformamide, and toluene and slightly soluble in hexanes.

SiPc[OSi(CH₃)₂(CH₂)₃N((CH₂)₄H)₂]₂, Pc 82, **21**. 61%. UV-vis (toluene) λ_{max}, nm (log ε): 669 (5.5). NMR (C₆D₆): δ 9.72 (m, 8H, 1,4-Pc H), 7.89 (m, 8H, 2,3-Pc H), 1.81 (t, 8H, NCH₂), 1.04 (m, 20H, NCH₂CH₂CH₂, Si(CH₂)₂CH₂), 0.80 (t, 12H, N(CH₂)₃CH₃), -0.89 (m, 4H, SiCH₂CH₂), -2.08 (m, 4H, SiCH₂), -2.61 (s, 12H, SiCH₃). HRMS-FAB (*m/z*): (M + H)⁺ calcd for C₅₈H₇₆N₁₀O₂Si₃, 1029.5539; found, 1029.5523, 1029.5511. **21** is a blue solid. It is soluble in CH₂Cl₂, dimethylformamide, and toluene and slightly soluble in hexanes.

SiPc[OSi(CH₃)₂(CH₂)₃N((CH₂)₅H)₂]₂, Pc 113, **22**. 48%. UV-vis (toluene) λ_{max}, nm (log ε): 669 (5.5). NMR (C₆D₆): δ 9.73 (m, 8H, 1,4-Pc H), 7.91 (m, 8H, 2,3-Pc H), 1.82 (t, 8H, NCH₂), 1.18 (m, 8H, NCH₂CH₂), 1.05 (m, 20H, N(CH₂)₂CH₂CH₂, Si(CH₂)₂CH₂), 0.83 (t, 12H, N(CH₂)₄CH₃), -0.87 (m, 4H, SiCH₂CH₂), -2.07 (t, 4H, SiCH₂), -2.60 (s, 12H, SiCH₃). HRMS-FAB (*m/z*): (M + H)⁺ calcd for C₆₂H₈₄N₁₀O₂Si₃, 1085.6165; found, 1085.6145, 1085.6134. **22** is a blue solid. It is soluble in CH₂Cl₂, dimethylformamide, and toluene and moderately soluble in hexanes.

SiPc[OSi(CH₃)₂(CH₂)₃N((CH₂)₆H)₂]₂, Pc 114, **23**. 36%. UV-vis (toluene) λ_{max}, nm (log ε): 669 (5.4). NMR (C₆D₆): δ 9.73 (m, 8H, 1,4-Pc H), 7.92 (m, 8H, 2,3-Pc H), 1.84 (t, 8H, NCH₂), 1.21 (m, 8H, NCH₂CH₂), 1.07 (m, 28H, N(CH₂)₂CH₂CH₂CH₂ and Si(CH₂)₂CH₂), 0.85 (t, 12H, N(CH₂)₅CH₃), -0.87 (m, 4H, SiCH₂CH₂), -2.07 (t, 4H, SiCH₂), -2.60 (s, 12H, SiCH₃). HRMS-FAB (*m/z*): (M + H)⁺ calcd for C₆₆H₉₂N₁₀O₂Si₃, 1141.6791; found, 1141.6774, 1141.6803. **23** is a blue solid. It is soluble in CH₂Cl₂, dimethylformamide, toluene, and hexanes.

Additional Phthalocyanines. SiPc[OSi(CH₃)₂(CH₂)₃NH₂]₂, Pc 38, **24**. Under Ar, a mixture of SiPc(OH)₂ (80 mg), 3-aminopropyltrimethylethoxysilane (0.80 g), and pyridine (200 mL) was distilled (~80 mL of distillate) for 30 min, concentrated by rotary evaporation (<35 °C), diluted with a H₂O–ethanol solution (2:1, 60 mL), and filtered. The solid was washed (H₂O–ethanol solution, 2:1), chromatographed (basic Al₂O₃ V, CH₂-Cl₂–ethyl acetate–triethylamine solution, 50:10:1), recrystallized twice (hexanes–CH₂Cl₂ solution, 10:1), washed (hexanes), air-dried, and weighed (64 mg, 58%). UV-vis (toluene) λ_{max}, nm (log ε): 668 (5.4). NMR (C₆D₆): δ 9.71 (m, 8H, 1,4-Pc H), 7.87 (m, 8H, 2,3-Pc H), 1.18 (t, 4H, Si(CH₂)₂CH₂), -1.16 (m, 4H, SiCH₂CH₂), -2.25 (t, 4H, SiCH₂), -2.64 (s, 12H, SiCH₃). HRMS-FAB (*m/z*): [M]⁺ calcd for C₄₂H₄₄N₁₀O₂Si₃, 804.2956; found 804.2979, 804.2980. **24** is a blue solid. It is soluble in CH₂Cl₂, dimethylformamide, and toluene and insoluble in hexanes.

GePc[OSi(*n*-C₆H₁₃)₃]₂. The synthesis of this compound has been described previously.⁶

NMR, UV–Visible Absorption, and Fluorescence Measurements. The NMR spectra were obtained with a Varian INOVA 400 MHz spectrometer (Varian Associates, Palo Alto, CA). The UV–vis spectra listed in the syntheses were recorded with a Perkin-Elmer Lambda 25 UV–vis spectrometer (Perkin-Elmer, Boston, MA). Steady state UV–vis spectra and the extinction coefficient of the compounds were obtained with a GBC 918 spectrophotometer using a 10 mm optical path length quartz cuvette at 25 °C. In each measurement, the sample was referenced to the background solvent (DMF) in a matched cuvette. Fluorescence spectra were monitored using a Spex Fluorolog 2 spectrofluorimeter ($\lambda_{\text{exc}} = 600$ nm) with 1.0 mm slits. All spectra were corrected for the sensitivity of the photomultiplier tube.

Flash Photolysis Experiments. Nanosecond flash photolysis studies were performed using a kinetic absorption spectrometer system that has been described previously.⁷ The excitation beam was a 6 ns pulse of 355 nm radiation obtained from a Surelite I (Continuum) Q-switched Nd:YAG pulsed laser (~60 mJ per pulse). For the experiments involved in the determination of triplet state lifetime measurements and transient absorption spectra, oxygen free samples in toluene solutions were required and thus the sample solutions were purged with argon or nitrogen for several minutes prior to excitation and a blanket of argon maintained over the solution during the experiment. The time profiles over the wavelength range 300–600 nm were recorded point by point at 10 nm steps, and the triplet state decay-kinetic profiles were recorded in the same fashion at 495 nm over the relevant time interval. The concentrations of the compounds were typically 2–3 μM , providing $A_{355} = 0.2$ – 0.25 in a 10 mm quartz cuvette.

For the determination of the bimolecular rate constants on oxygen quenching of the triplet states, the solutions were saturated in turn with air, argon, and oxygen by bubbling the samples with the appropriate gas for several minutes in a cuvette with a Teflon cap equipped with a hypodermic syringe and a small hole to allow egress of gas.

Singlet Oxygen Quantum Yields. Singlet oxygen emission spectra from the phthalocyanine samples in toluene were obtained using a Bruker ISF 55 FTNIR spectrometer modified to operate in the emission mode. All measurements were carried out at room temperature in air-saturated solutions. A liquid-N₂-cooled (77 K) Ge detector/amplifier combination (Applied Detector Corp., model 403HS) was used to monitor the near-IR signals. Sample excitation was accomplished with the 633 nm line of a 50 mW He–Ne laser (Spectra Physics, model 127), using an optical fiber to direct the excitation beam to the cuvette. The luminescence signal was detected at right angles via an AR-coated silicon metal filter of the germanium photodiode amplifier unit operated at 77 K. Spectra were recorded at a resolution of 64 cm⁻¹, and the final spectra were obtained by averaging 256 individual scans. The diameter of the aperture was 10 mm. The integration limits were defined by the first minima of the signal on both sides of the emission peak. The baseline was defined by the line connecting the two points at which the signal crosses the integration borders. By defining the baseline as well as the integration limits in such manner, it was possible to reduce the error of the integrated value of the emission signal introduced by noise in the baseline region. Thus, the integrated areas, G_{Δ} , of the near-IR luminescence signal (at 1270 nm) of the singlet oxygen generated from toluene solutions of phthalocyanine compounds were compared to that produced

from an optically matched solution of tetraphenylporphyrin (TPP) ($A_{633} = 0.55$) in toluene for which the singlet oxygen quantum yield is known, $\Phi_{\Delta}^{\text{REF}} = 0.58$.⁸

The singlet oxygen quantum yields were evaluated according to

$$G \propto B(1/\tau_{\Delta})\eta_{\Delta}\Phi_{\Delta}E(1 - 10^{-A})$$

where η_{Δ} is the fraction of the triplet states that are quenched by O₂, Φ_{Δ} is the quantum yield of singlet oxygen, B is an instrument factor, A is the absorbance at the 633 nm excitation wavelength, τ_{Δ} is the intrinsic lifetime of the singlet oxygen in toluene (a constant in the same solvent), and E is the incident photon rate. Under identical excitation and absorbance conditions, the quantities B , τ_{Δ} , Φ_{Δ} , E , and absorbance ($1 - 10^{-A}$) are constant. Thus, the quantum yields of singlet oxygen could be computed according to

$$\Phi_{\Delta}^{\text{Pc}} = \Phi_{\Delta}^{\text{REF}} \frac{G_{\Delta}^{\text{Pc}}}{G_{\Delta}^{\text{REF}}} \times \frac{\eta_{\Delta}^{\text{REF}}}{\eta_{\Delta}^{\text{Pc}}}$$

where η_{Δ} is the fraction of donor triplet states scavenged by oxygen at air saturation and is given by

$$\eta_{\Delta} = \frac{k_{\text{Q}}[{}^3\text{O}_2]}{k_0 + k_{\text{Q}}[{}^3\text{O}_2]}$$

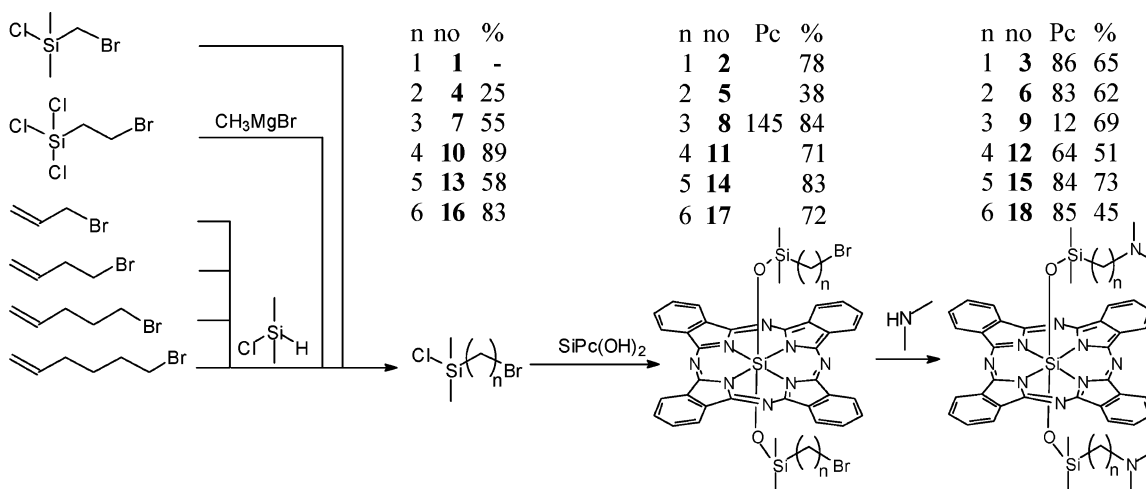
where k_0 is the rate constant of the triplet state decay in the absence of oxygen, k_{Q} is the bimolecular rate constant for oxygen quenching, and $[{}^3\text{O}_2]$ is the oxygen concentration in the air-saturated toluene solution.

Fluorescence Lifetime Measurements. Fluorescence lifetime measurements were carried out with a time resolved single photon counting instrument from Edinburgh Analytical Instruments (FL/FS 900). Excitation was performed with a nanosecond flash lamp (nF 900) operating under an atmosphere of H₂ gas (0.5–0.55 bar, 0.7 nm fwhm, 40 kHz repetition rate). Most of the samples were excited at 355 nm (Pc 84, Pc 85, and Pc 38 were excited at 663.0 nm) in air-saturated benzene or toluene solutions, and the fluorescence decay was monitored at 682.0 nm. The output of the nanosecond flash lamp was passed through a monochromator, and emission was collected at 90° and passed through a second monochromator. A Peltier-cooled (–30 °C) red sensitive photomultiplier tube (PMT), R955, was used to register the emission. The temperature of the sample was maintained at 25 ± 1 °C for all measurements by means of a Neslab RTE-111 circulating bath. The excitation wavelength at 355 nm was chosen so that the absorbance of each sample was 0.06–0.1 per cm at the excitation wavelength for all of the solutions containing phthalocyanine compounds. The TRSPC procedure using this system has been described.⁹ The data were analyzed by deconvolution of the emission decay profile with the instrument response function using software provided by Edinburgh Instruments.

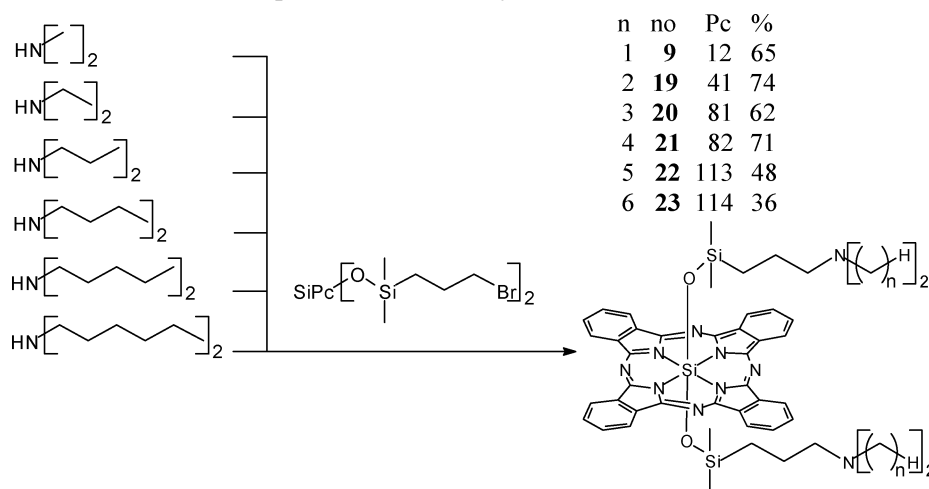
Results and Discussion

Synthesis. The reactions used to prepare the linker-group phthalocyanines, series 1 (Figure 1), are summarized in Scheme 1. Hydrosilylation reactions such as that used for ligand **7** gave ligand **4** in low yield at moderate temperatures (<50 °C) and the α -bromo isomer of ligand **4** at higher temperatures. The use of a more suitable catalyst might have given ligand **4** in good yield. The Grignard synthesis used for ligand **4** was reliable

SCHEME 1: Syntheses of Linker-Group, Series 1, Phthalocyanines



SCHEME 2: Syntheses of Terminal-Group, Series 2, Phthalocyanines



but required careful control of the reaction conditions because of the susceptibility of both ligand **4** and the reaction intermediate $\text{Cl}_2\text{SiCH}_3(\text{CH}_2)_2\text{Br}$ to β -elimination as a result of nucleophilic attack by base (CH_3^-).¹⁰ Tetrahydrofuran worked well as a reaction solvent for the amination reactions. Clearly, the route used for linker phthalocyanine **9** and its three higher linker homologues is general and can be used for still higher homologues. The procedures used for all six linker phthalocyanines are straightforward and reliable. Alternative routes reported for **9**^{11–13} are less preferable.

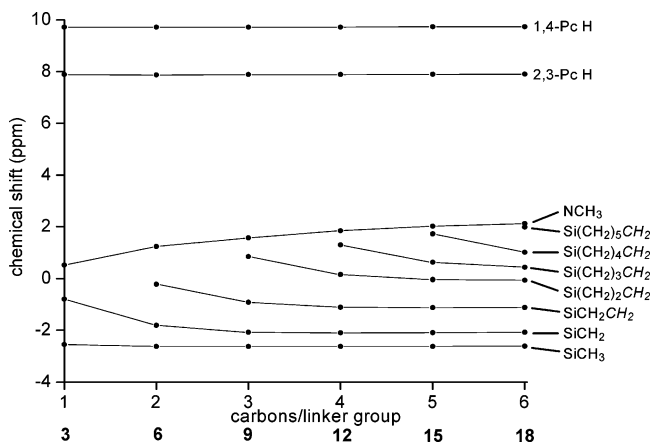


Figure 2. Positions of the NMR resonances of the linker-group, series 1, phthalocyanines in C_6D_6 .

The positions of the NMR resonances of intermediate phthalocyanine **2** and its homologues and of linker phthalocyanine **3** and its homologues show that extension of the linker chain and exchange of the bromo group for the amino group cause only relatively small shifts of the common resonances of the compounds (Figure 2). The shifts observed are understandable in terms of electronegativity and ring-current effects.

The reactions used for the terminal-group phthalocyanines, series 2 (Figure 1), are summarized in Scheme 2. All make use of intermediate phthalocyanine **8** and of an excess of the amine reactant as the reaction solvent. All reactions are simple, straightforward, and reliable. With the amino compound **9**, which is common to the two sets of compounds and is important because it can be used to make the PDT drug Pc **4**,¹¹ the use of excess dimethylamine as the reaction solvent instead of tetrahydrofuran offers the advantage of easier product isolation. The variations in the positions of the common resonances of the terminal-group compounds (Figure 3) are again interpretable in terms of electronegativity and ring-current effects. The synthesis used for $\text{SiPc}[\text{OSi}(\text{CH}_3)_2(\text{CH}_2)_3\text{NH}_2]_2$, Pc **38**, is attractive because both of the reactants are readily available. The NMR resonances of this phthalocyanine are as expected.

Ground State Absorption Spectra. The UV–vis absorption spectra of the phthalocyanine compounds studied in the photo-physical work were measured in DMF solutions. All showed similar spectral behavior, and the spectrum shown in Figure 4 for Pc **12** is typical. There, it is seen that the Q band peak of Pc

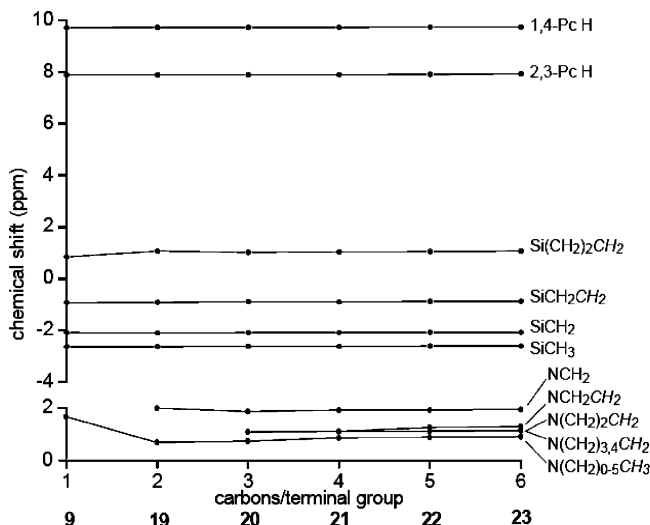


Figure 3. Positions of the NMR resonances of (upper) phthalocyanine and siloxy protons and (lower) amino protons of the terminal-group, series 2, phthalocyanines in C₆D₆.

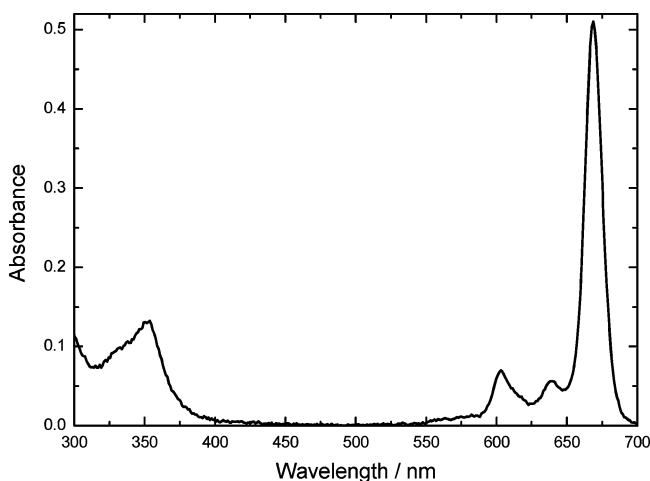


Figure 4. UV-visible absorption spectrum of the ground state of Pc 12 (2.5 μM).

12 has a vibronic progression with an intense narrow red-most peak at 669 nm and a B band peak at 352 nm. All compounds showed the same (± 1 nm) B band and Q band maxima. Extinction coefficients at the Q band peak (668.5 nm) were grouped near $3 \times 10^5 \text{ M}^{-1} \text{ cm}^{-1}$ (see Synthesis section). Beer-Lambert law plots for all of the compounds showed excellent linearity in the range of concentrations investigated (up to 20 μM), indicating no evidence for aggregation in the ground state.

The vibronic sequence in the Q bands of phthalocyanine-type compounds of D_{4h} or approximately D_{4h} symmetry is well-known¹⁴⁻¹⁶ and is attributed to an electronic transition ($S_0 \rightarrow S_1$) between a filled π molecular orbital (e.g., HOMO) and a pair of empty, higher energy, doubly degenerate π^* molecular orbitals (a_{1u} , LUMO).¹⁷ Moreover, for the compounds of clearly lower symmetry than D_{4h} , splitting of the Q band is commonly observed¹⁸ and is attributed to a similar kind of $\pi-\pi^*$ transition ($S_0 \rightarrow S_1$), where the π^* orbitals are now nondegenerate owing to the lower symmetry. All members of both series, SiPc[OSi(CH₃)₂(CH₂)_{*n*}N(CH₃)₂] and SiPc[OSi(CH₃)₂(CH₂)₃N((CH₂)_{*n*}H)₂]₂, showed this single vibronic sequence and are thus of approximately D_{4h} symmetry (Figure 1). The NMR spectra (Figures 2 and 3) support this conclusion.

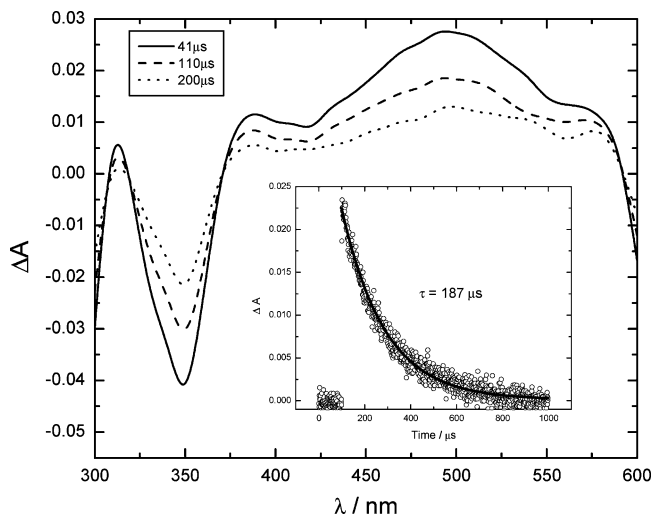


Figure 5. Transient absorption spectra of Pc 83 recorded at three different times (as shown) after pulsed irradiation of an $\sim 3.8 \mu\text{M}$ solution in toluene at room temperature. The inset shows the exponential decay at 495 nm.

TABLE 1: Phthalocyanine Triplet State Lifetimes, τ_T , in N₂-Saturated Toluene; Bimolecular Rate Constants of Triplet State Quenching by Oxygen, k_q ; and Singlet Oxygen Quantum Yields, Φ_Δ , in Air-Saturated Toluene

compound	($\tau_T \pm 10$), μs	$10^9 k_q$, M ⁻¹ s ⁻¹	Φ_Δ
Pc 86	236	2.48	0.16
Pc 83	187	2.96	0.17
Pc 12	181	2.18	0.26
Pc 64	170	2.85	0.36
Pc 84	173	2.39	0.36
Pc 85	235	2.42	0.35
Pc 38	160	3.01	0.40
Pc 41	181	2.8	0.09
Pc 81	178	3.1	0.02
Pc 82	229	2.3	0.02

Triplet States: Transient Spectra and Kinetics. Pulsed laser excitation at 355 nm of deaerated toluene solutions of all of the members of the two series except Pc 113 and Pc 114 leads to transient absorbance spectra such as those shown in Figure 5 (for Pc 83). A representative time profile is included as an inset in this figure. All compounds studied showed similar spectral features, namely, negative absorption (bleaching) in the Soret region and above 575 nm and a broad positive absorption centered near 500 nm. Isosbestic points were detected at ~ 369 nm and ~ 590 nm. Under the prevailing conditions of argon saturation, the absorption features (positive and negative) of all compounds investigated recovered to the prepulse zero level exponentially (Figure 5), with relatively similar lifetimes, $\tau = 198 \pm 38 \mu\text{s}$, as tabulated in Table 1. The observations that the bleaching recovery and absorption decay kinetics are closely similar and that the different spectral regions are separated by isosbestic points, are indicative of concomitant processes. It is therefore concluded that the photo-generated transient is decaying to repopulate the ground state material in a single exponential process (Figure 5). Other p-block metal phthalocyanines studied in this laboratory^{19,20} show similar transient spectral and temporal behavior, and the immediate precursor of the repopulated ground state has been concluded to be the triplet state of the compounds. Thus, the observed positive broad absorption centered at ~ 495 nm, decaying exponentially to zero baseline (*vs.*) for all of the members of both series studied, is assigned to the $T_1 \rightarrow T_n$ transition.

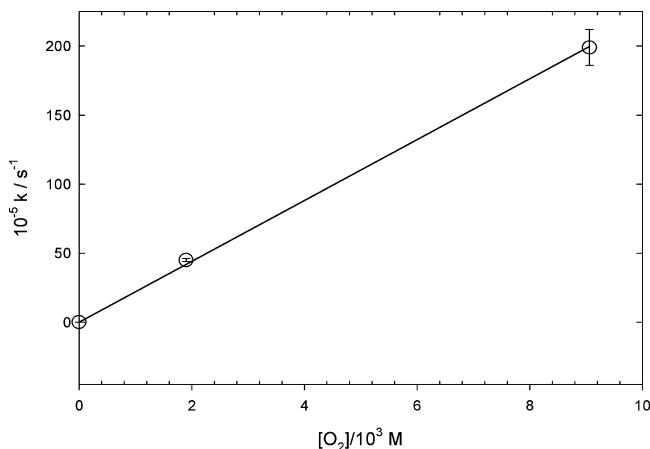


Figure 6. Competition plot of the dependence of the first-order decay rate constant of the triplet state of Pc 12 by oxygen at room temperature in toluene.

TABLE 2: Comparison of Fluorescence Lifetimes and Singlet Oxygen Yields

compound	Φ_{Δ}	τ_i , ns (%)	$\Delta A_{495} (t=0)$
Pc 86	0.16		
Pc 83	0.17	$\tau_1 = 1.5$ (49.0); $\tau_2 = 5.0$ (51.0)	
Pc 12	0.26	$\tau_1 = 1.51$ (84.3); $\tau_2 = 5.3$ (15.7)	
Pc 64	0.36	$\tau = 5.0$	0.036
Pc 84	0.36	$\tau = 6.0$	
Pc 85	0.35	$\tau = 6.7$	
Pc 38	0.40	$\tau = 7.0$	
Pc 41	0.09	$\tau_1 = 0.9$ (17.1); $\tau_2 = 4.7$ (82.9)	
Pc81	0.02	$\tau_1 = 0.4$ (86.7); $\tau_2 = 5.0$ (13.3)	0.008
Pc82	0.02	$\tau_1 = 0.4$ (85.7); $\tau_2 = 4.9$ (14.3)	0.008

Absolute quantum yields of the triplet state of series 1 and 2 were not explicitly measured. Nonetheless, the relative yield could be estimated from the initial transient absorbance (at 495 nm), $\Delta A_{t=0}$, for the optically matched solutions of Pc 64, Pc 81, and Pc 82 (Table 2). In comparison to the $\Delta A_{t=0}$ value of 0.036 for Pc 64 (a member of series 1), smaller $\Delta A_{t=0}$ values for Pc 81 and Pc 82 (series 2), namely, 0.008, were obtained. Thus, assuming that the extinction coefficient for the T–T transition, ϵ_{495} , is approximately constant for all of the members of the series, the triplet yield of Pc 64 must be significantly higher than those of Pc 81 and Pc 82. This has consequences on the quantum yields of singlet oxygen generated from the triplet states, as revealed below.

Oxygen Quenching of the Triplet States. The triplet states of all compounds decayed more rapidly in the presence of increasing oxygen concentration in a first-order manner with respect to O_2 concentration. Plots of the measured first-order rate constants against oxygen concentration were linear (Figure 6) whence bimolecular rate constants for oxygen quenching, k_q , were evaluated. The values are collected in Table 1 and are all in the range $(2-3) \times 10^9 M^{-1} s^{-1}$, as anticipated^{6,19} for the oxygen quenching of a triplet state where the energy transfer process is exergonic.

Singlet Oxygen Quantum Yields. To determine whether oxygen quenching of the Pc triplet states leads to the formation of singlet oxygen, $O_2 (^1\Delta_g)$, a steady state technique was employed to measure the singlet oxygen yields in air-saturated toluene solutions. This is based on the observation of the near-infrared emission of $^1\Delta_g$ at 1270 nm. Figure 7 shows spectra of the $O_2 (^1\Delta_g, v=0) \rightarrow O_2 (^3\Sigma_g^-, v=0)$ transition for all compounds studied, optically matched at 633 nm ($A = 0.55$). The singlet oxygen luminescence of an optically matched toluene solution of tetraphenylporphyrin (TPP) is also plotted

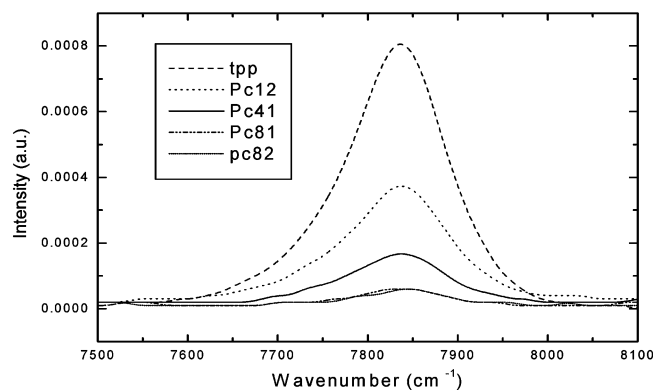
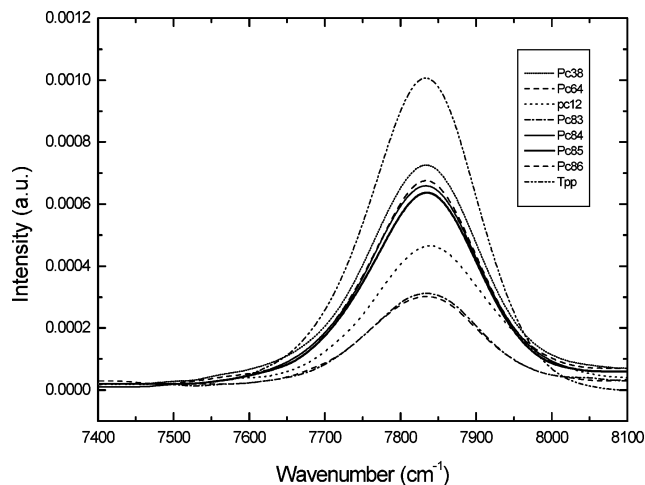


Figure 7. (upper panel) Singlet oxygen emission spectra in toluene for the series of phthalocyanines, TPP, Pc 38, 64, 84, 85, 12, 86, and 83. (lower panel): State singlet oxygen emission spectra in toluene for the series of compounds, TPP, Pc 12, 41, 81, and 82.

in the same graph. The quantum yields were evaluated using the following expression from the Experimental Section:

$$\Phi_{\Delta}^{\text{Pc}} = \Phi_{\Delta}^{\text{REF}} \frac{G_{\Delta}^{\text{Pc}}}{G_{\Delta}^{\text{REF}}} \times \frac{\eta_{\Delta}^{\text{REF}}}{\eta_{\Delta}^{\text{Pc}}}$$

In this computation, the values of η_{Δ} for all compounds and for TPP were found to be unity. The collected data are presented in Table 1. Discussion of these data is presented below.

In addition to the singlet oxygen emission peak at 7800 cm^{-1} , a spectral wing of lower intensity ($\sim 8\times$) at $\sim 6250 \text{ cm}^{-1}$ ($\sim 1600 \text{ nm}$) and another weakly resolved feature was observed at $\sim 8775 \text{ cm}^{-1}$ (1140 nm) for most compounds investigated. A representative near-IR spectrum observed for Pc 64 with these spectral features is shown in Figure 8. The spectral feature at $\sim 6250 \text{ cm}^{-1}$ ($\sim 1600 \text{ nm}$) is assigned to²¹ the $v'=0 \rightarrow v=1$ transition in O_2 . The observed weakly resolved near-IR (NIR) band at $\sim 1140 \text{ nm}$ in air-saturated solutions that was enhanced upon argon saturation and disappeared upon oxygen saturation (replaced by the 7800 cm^{-1} band of $O_2 (^1\Delta_g)$) was assigned to phthalocyanine phosphorescence.^{18,21} On the basis of this observation, the triplet state energies of the phthalocyanines were calculated to be approximately 25 kcal mol^{-1} .

Fluorescence Lifetime Measurements. The fluorescence lifetimes of several compounds were measured using time-correlated single photon counting (TRSPC). Solutions in toluene were excited at 355 nm, and the fluorescence time profiles at 680 nm were monitored. The fluorescence lifetimes of all of the members of the two series (except Pc 86) are listed in Table

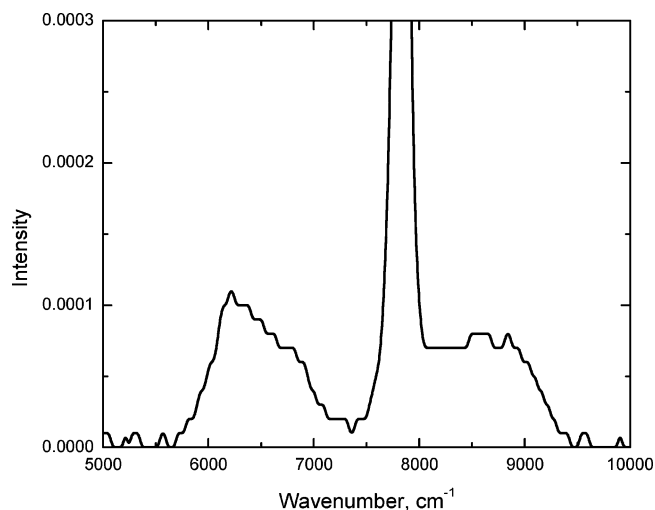


Figure 8. NIR signal for Pc 64 in toluene indicating 0,1 transition of singlet oxygen luminescence ($\sim 6250\text{ cm}^{-1}$) and overlapping phosphorescence band ($\sim 8775\text{ cm}^{-1}$).

2 along with singlet oxygen yields. The lifetime of Pc 86 was not obtained due to the instability of the sample as noted by the change in the ground state absorption spectrum during the experimental runs.

Comparison of Fluorescence Lifetimes and Singlet Oxygen Yields. The fluorescence time profiles of compounds Pc 64, Pc 84, Pc 85, and Pc 38 showed single exponential decay and lifetimes of $6 \pm 1\text{ ns}$. The fluorescence time profiles of all of the other compounds (Pc 83, 12, 41, 81, and 82) were best fit as sums of two exponentials (Table 2), with components of shorter lifetimes ($1.5\text{ ns} \rightarrow 0.4\text{ ns}$) and longer lifetime ($\sim 5\text{ ns}$) components; see Table 2. The compounds Pc 41, 81, and 82 have tertiary amino termini and linkers containing three methylene units. It is known that tertiary, and other, amines are effective electron donors and are known to act as excited state quenchers.²² As Figure 1 indicates, the amino termini of the axial ligands of the compounds investigated are tethered to the central Si atom of the phthalocyanine π -systems by methylene linker chains of variable length (one to six CH_2 units). Thus, upon photoexcitation, the $^1\pi,\pi^*$ state of the phthalocyanine residue and a putative quenching amino residue are in relative proximity because of the tether linking them. The tether is solely a σ -bonded skeleton and is therefore flexible, allowing a multiplicity of conformational states to be visited by the electron donor entity (the amine) and the S_1 state of the π -system (the putative acceptor). Thus, the intrinsic structure of the molecule and the flexible nature of the linkers convey the possibility of an intramolecular charge transfer quenching process, perhaps via the formation of an intramolecular exciplex. Such quenching introduces an additional deactivation channel for Pc(S_1), an addition that will serve to reduce the quantum efficiency of triplet state formation, as noted above. From the variability of the fluorescence lifetime data, it is clear that the additional deactivation channel is not constant from one phthalocyanine to the next. For Pc 64, Pc 84, and Pc 85, the decays were single exponential with lifetimes near 6 ns, which presumably represents the unquenched value. In these compounds, the linkers contain four, five, and six methylene units, respectively, and the tethered dimethylamino termini are relatively remote from the π -system and therefore are able to explore a greater number of nonquenching conformational states than those compounds with linkers of three methylene residues and less. In other words, the time required for the system to diffuse to a conformation that allows quenching to occur is too long with respect to the

intrinsic lifetime of the singlet states and therefore the additional intramolecular quenching channel is effectively closed. The fluorescence lifetime data reveal that this channel becomes open for Pc 83, 12, 41, 81, and 82, compounds showing biexponential fluorescence time profiles. These compounds have three or less methylene residues in the linker, and employing the above argument, now there are fewer conformational states and therefore the probability of the system diffusing to a reactive one within the intrinsic lifetime of S_1 is sufficiently high that the intramolecular deactivation channel opens up, at least for some molecules in the excited ensemble. The fact that the longer lifetime component in these five compounds is close to the unquenched value can be interpreted to the effect that in the excited state ensemble a fraction of the excited states are unable to achieve the quenching conformation(s) and these thus contribute the longer lifetime component; the remaining fraction are able to do this and thus contribute the short-lived component.

This may not be the whole story because scrutiny of Table 2 shows that the short lifetime component decreases with lengthening of the alkyl chain length in the alkylamino termini. This effect seems to be a variance with the conformational diffusion model discussed above, as one would expect the bulkier alkylamino residues to move more slowly, thereby providing longer lifetime short-lived components. It is not inconceivable that there is an “entanglement factor” in play whereby the longer alkyl chains, through hydrophobic interactions, encourage close approach between the donor termini and the π -system in the ground state molecule, thereby generating preformed quenching pairs. The resolution of these different viewpoints must await more pertinent data. Additionally, Pc 38 is a special case, since it has $n = 3$ methylene residues in the linker but also has a single exponential 7 ns lifetime fluorescence. Presumably this arises because its primary amine terminus has a significantly weaker donating power²⁴ compared to the tertiary amine termini carried by the other analogues. Even though putative quenching conformational states can be visited ($n = 3$) during the S_1 lifetime, the lower donating power creates an energy barrier to the quenching process. The donor properties of amines are of considerable practical interest for the photoreduction of various chromophores including ketones,²³ azoalkanes,²⁴ and dyes.²⁵

The above mechanistic arguments are supported by the singlet oxygen quantum yields. According to the Φ_Δ values presented in Table 1, the compounds Pc 64, 84, 85, and 38 show singlet oxygen yields ≥ 0.35 , here called the “normal” range. These phthalocyanines possess axial ligands that are terminated by dimethylamino residues at the end of four or more methylene units (Pc 64, 84, and 85), or by a primary amine residue (Pc 38). These are the same compounds discussed above that show single exponential fluorescence time profiles; that is, no quenching conformational states are visited during the S_1 lifetime; therefore, triplet quantum efficiencies and, by turn, the singlet oxygen yields are optimal. Compounds Pc 12, 86, and 83 have shorter linkers (three or less methylene links) terminated by dimethylamino termini, and these display intermediate singlet oxygen quantum yields (0.16–0.26). Of these, Pc 12 and Pc 83 have biexponential fluorescence decay (Pc 86 could not be measured, as noted above) with a dominant fast component of 1.5 ns. This conveys the idea of an intermediate degree of phthalocyanine S_1 state quenching, leading to singlet oxygen yields of somewhat less than normal. The Φ_Δ values for compounds Pc 41, 81, and 82 were significantly lower (< 0.1). These last are those that show a less than 1 ns fast component in their fluorescence time profiles, and therefore, the S_1 states

are significantly quenched with consequent reductions in triplet and singlet oxygen yields.

Thus, the variability in the singlet oxygen quantum yields, in the relative triplet yields, and in the fluorescence lifetime data leads to the conclusion that in some cases the nitrogen atom of the terminal amine residues is able to electronically interact with the photogenerated S_1 state of the phthalocyanine during its 6 ns lifetime. It is the effectiveness of this interaction that leads to partial quenching of the excited state and in turn lower triplet yields and lower singlet oxygen yields. It is very likely that the nature of the interaction can be described as intramolecular charge transfer between tethered donor and acceptor moieties undergoing restricted diffusion through an ensemble of conformational states. It is not inconceivable that the charge transfer interaction involves the formation of an intramolecular exciplex. Such entities have been reported,²⁶ and our results are of those reported for fluorescence quenching of naphthyl units of 1,4,8,11-tetraazacyclotetradecane (cyclam) via intramolecular exciplex formation with the cyclam nitrogen atoms.²⁷ However, at this time, evidence of exciplex formation is lacking in the Pc–amine interaction investigated here.

Concluding Remarks

The routes used to prepare the silicon phthalocyanines having axial siloxy ligands terminating in alkylamino groups are reliable and provide a good basis for the synthesis of similar compounds. The NMR spectra of these compounds show no unexpected features and can be interpreted in a straightforward way. The similarities in the structure of these compounds led to an expectation that their photophysical properties would be very similar. It was therefore intriguing to first find a strong variation in singlet oxygen quantum yields, then in triplet yields, and finally in Pc fluorescence behavior. It finally became clear that the terminal amine residues on the axial ligands were able to quench the Pc S_1 state on account of their relative proximity, and the extent of this quenching, perhaps via an intramolecular exciplex, depended critically on the chemical nature of the amine residues and on the length of the tether.

Acknowledgment. This research has been supported in part by NIH grants CA 91027, CA 46281, and CA 48535 and by the Center for Photochemical Sciences at Bowling Green State University. H.M.A. is grateful to the McMaster Foundation at BGSU for a predoctoral fellowship. We thank Dr. F. N. Castellano for the use of the time-correlated single photon counting instrument and for guidance with data analysis. We are grateful to Dr. G. Hao for providing some of the samples used to obtain the mass spectra and to Mr. Mikhail Chamachkine for instrumental assistance. We also wish to acknowledge Drs. Anthony A. Gorman and Kevin Henbest for many helpful discussions throughout this project.

References and Notes

- (1) Kanofsky, J. R. *Chem.-Biol. Interact.* **1989**, *70*, 1.
- (2) Weishaupt, K. R.; Gomer, C. J.; Dougherty, T. J. *Cancer Res.* **1976**, *36*, 2326.
- (3) Kessel, D.; Dutton C. J. *Photochem. Photobiol.* **1984**, *40*, 403.
- (4) (a) Ben Hur, E.; Rosenthal, I. *Photochem. Photobiol.* **1985**, *42*, 129. (b) Spikes, J. D. *Photochem. Photobiol.* **1986**, *43*, 691. (c) Brasseur, N.; Ali, H.; Langlois, R. Van Lier, J. E. *Photochem. Photobiol.* **1985**, *42*, 515.
- (5) Berlin, J. C. Ph.D. Thesis, Case Western Reserve University, Cleveland, OH, 2006.
- (6) Pelliccioli, A. P.; Henbest, K.; Kwag, G.; Carvagno, T. R.; Kenney, M. E.; Rodgers, M. A. J. *J. Phys. Chem. A* **2001**, *105*, 1757–1766.
- (7) Ford, W. E.; Rodgers, M. A. J. *J. Phys. Chem.* **1994**, *98*, 3822.
- (8) Rossbroich, G.; Garcia, N. A.; Braslavsky, S. E. *J. Photochem.* **1985**, *37*, 31.
- (9) Tyson, D. S.; Castellano, F. N. *J. Phys. Chem. A* **1999**, *103*, 10955.
- (10) Sommer, L. H.; Bailey, D. L.; Goldberg, G. M.; Buck, C. E.; Bye, T. S.; Evans, F. J.; Whitmore, F. C. *J. Am. Chem. Soc.* **1954**, *76*, 1613–1618.
- (11) Oleinick, N. L.; Antunez, A. R.; Clay, M. E.; Rihter, B. D.; Kenney, M. E. *Photochem. Photobiol.* **1993**, *57*, 242–247.
- (12) Kenney, M. E.; Oleinick, N. L.; Rihter, B. D.; Li, Y.-S. U.S. Patent 5,484,778, Jan 16, 1996.
- (13) He, J.; Larkin, H. E.; Li, Y.-S.; Rihter, B. D.; Zaidi, S. I. A.; Rodgers, M. A. J.; Mukhtar, H.; Kenney, M. E.; Oleinick, N. L. *Photochem. Photobiol.* **1997**, *65*, 581–586.
- (14) Solovev, K. N.; Mashenkov, V. A.; Kachura, T. F. *Opt. Spectrosc. (Engl. Transl.)* **1969**, *27*, 24.
- (15) Konami, H.; Ikeda, Y.; Hatano, M.; Mochizuki, K. *Mol. Phys.* **1993**, *80*, 153.
- (16) Linssen, T. G.; Hanack, M. *Chem. Ber.* **1994**, *127*, 2051.
- (17) Leznoff, C. C.; Lever, A. B. P., Eds. *Phthalocyanines: Properties and Applications*; VCH Publishers: New York, 1996; Vol. I, 1989; Vols. II and III, 1993.
- (18) (a) Kane, A. R.; Sullivan, J. F.; Kenney, D. H.; Kenney, M. E. *Inorg. Chem.* **1970**, *9*, 1445. (b) Hush, N. S.; Woolsey, I. S. *Mol. Phys.* **1970**, *21*, 465.
- (19) (a) Rihter, B. D.; Kenney, M. E.; Ford, W. E.; Rodgers, M. A. J. *J. Am. Chem. Soc.* **1990**, *112*, 8064. (b) Nikolaitchik, A. V.; Rodgers, M. A. J. *J. Phys. Chem. A* **1999**, *103*, 7597. (c) Firey, P. A.; Ford, W. E.; Sounik, J. R.; Kenney, M. E.; Rodgers, M. A. J. *J. Am. Chem. Soc.* **1988**, *110*, 7626.
- (20) Aoudia, M.; Cheng, G.; Kennedy, V. O.; Kenney, M. E.; Rodgers, M. A. J. *J. Am. Chem. Soc.* **1997**, *119*, 6029–6039.
- (21) Wessels, J. M.; Rodgers, M. A. J. *J. Phys. Chem.* **1995**, *99*, 17586.
- (22) (a) Cohen, S. G.; Parola, A.; Parsons, G. H. Jr. *Chem. Rev.* **1973**, *73*, 141. (b) Scaiano, J. C. *J. Photochem.* **1973**, *2*, 81. (c) Griller, D.; Howard, J. A.; Marriot, P. R.; Scaiano, J. C. *J. Am. Chem. Soc.* **1981**, *103*, 619.
- (23) (a) Miyasaka, H.; Mataga, N. *Bull. Chem. Soc. Jpn.* **1990**, *63*, 131. (b) Scaiano, J. C. *J. Photochem.* **1973**, *2*, 81–118
- (24) Adam, W.; Moorthy, J. N.; Nau, W. M.; Scaiano, J. C. *J. Org. Chem.* **1996**, *61*, 8722.
- (25) Timpe, H. J.; Jockusch, S.; Korner, K., Eds. *Dye Sensitized Photopolymerization*; Elsevier: London, 1993; Vol. II.
- (26) (a) Speiserr, S. *Chem. Rev.* **1996**, *96*, 1953 and references therein. (b) Galindo, F.; Jiminez, M. C.; Miranda, M. A.; Tormos, R. *Chem. Commun.* **2000**, 1747. (c) Roy, M. B.; Ghosh, S.; Bandyopadhyay, P.; Bharadwaj, P. K. *J. Lumin.* **2000**, *92*, 115. (d) Zhou, Q.; Swager, T. M. *J. Am. Chem. Soc.* **1995**, *117*, 12593. (e) Ashton, P. R.; Ballardini, R.; Balzani, V.; Belohradsky, M.; Gandolfi, M. T.; Philp, D.; Prodi, L.; Raymo, F. M.; Reddington, M. V.; Spencer, N.; Stoddart, J. F.; Venturi, M.; Williams, D. J. *J. Am. Chem. Soc.* **1996**, *118*, 4931. (f) Chandrasekharan, N.; Kelly, L. A. *J. Am. Chem. Soc.* **2001**, *123*, 9898. (g) Lakowicz, J. R. *Topics in Fluorescence Spectroscopy*; Kluwer Academic/Plenum Publishers: New York, 2000; Vol. 6.
- (27) Saudan, C.; Balzani, V.; Gorka, M.; Lee, S.; Maestri, M.; Vicinelli, V.; Vogtle, F. *J. Am. Chem. Soc.* **2003**, *125*, 4424.